Do Existing Theories Explain Seasonal to Multi-Decadal Changes in Glacier Basal Sliding Speed?

F Gimbert, A Gilbert, O Gagliardini, C Vincent, L Moreau

Geophysical Research Letters

RESEARCH LETTER
10.1029/2021GL092858

Special Section:
Modeling in glaciology

Do Existing Theories Explain Seasonal to Multi-Decadal Changes in Glacier Basal Sliding Speed?

F. Gimbert[1], A. Gilbert[1], O. Gagliardini[1], C. Vincent[1], and L. Moreau[2]

[1]Université Grenoble Alpes, CNRS, IGE, Grenoble, France, [2]Edytem, CNRS, Université de Savoie, Chambéry, France

Key Points:

- We use unique basal sliding observations collected over three decades to test basal friction theories
- The observations show striking agreement with theory, although we report an unexpected stress stabilization near Iken's limit
- Stress stabilization causes basal effective pressure to scale with bed shear stress, and long-term sliding speeds to follow a simple law

Supporting Information:

Supporting Information may be found in the online version of this article.

Correspondence to:

F. Gimbert,
florent.gimbert@univ-grenoble-alpes.fr

Citation:

Gimbert, F., Gilbert, A., Gagliardini, O., Vincent, C., & Moreau, L. (2021). Do existing theories explain seasonal to multi-decadal changes in glacier basal sliding speed? *Geophysical Research Letters*, *48*, e2021GL092858. https://doi.org/10.1029/2021GL092858

Received 15 FEB 2021
Accepted 21 JUN 2021

Abstract Theoretical descriptions of ice-bed friction beneath glaciers and ice sheets are key to predict changes in sea level. Applicability of these theories at the natural landscape scale and over long periods has however not been tested. Here we test hard bed friction laws by analyzing a unique data set of in-situ basal sliding measurements collected over three decades under an Alpine glacier enduring large changes in geometry. We report many observational features that are in striking agreement with theoretical predictions. However, we also observe an undocumented behavior where the basal stress state stabilizes near Iken's limit under meltwater input, which suggests the basal effective pressure is primarily set by bed shear stress rather than by water input and drainage specifics as commonly thought. As a result, long-term changes in year-averaged sliding velocities follow a simple power law scaling with bed shear stress as opposed to more complex pressure-dependent relationships.

Plain Language Summary Basal sliding is an important component of glacier motion. However, our knowledge of the physics that controls basal sliding is incomplete. This causes large uncertainties in the contribution to sea-level rise predicted for ice sheets over the coming century. Here, we test our understanding of basal sliding against particularly unique observations, made via a rotating bicycle wheel that has been continuously measuring glacier basal motion over three decades within excavated tunnels under the Argentière Glacier in the French Alps. Due to stress changes from significant glacier thinning over the multi-decadal period we are able to establish an observationally derived sliding law and compare it with expectations from theory. We report many observational features that are in striking agreement with theoretical predictions from glacier sliding over bedrock beds. However, we also observe an undocumented behavior of stress stabilization during the melting period at a specific stress state known as the Iken's limit. This behavior causes long term sliding velocities to follow a simple power law scaling with bed shear stress. This finding has the potential of strongly simplifying and reducing uncertainty on predicting glaciers response to climate change.

1. Introduction

Physically based sliding laws for glaciers over a hard (non-deformable) bed (Fowler, 1986, 1987; Gagliardini et al., 2007; Schoof, 2005; Weertman, 1957) rely on simplifying assumptions originally proposed by Weertman (1957) and Lliboutry (1959, 1968). On one hand, the ice-bed contact is assumed as frictionless and thus basal friction occurs at a meso-scale (centimeters to few tens of meters) due to ice flow around bed irregularities via enhanced creep and pressure melting mechanisms (Weertman, 1957). With this consideration, one neglects the effect of other sliding mechanisms inferred to operate near or at the ice-bed interface, such as ice fracturing (Walter et al., 2013) or basal stick-slip (Helmstetter, Nicolas, et al., 2015; Lipovsky et al., 2019; Smith, 2006). On the other hand, subglacial hydrology is considered to modulate basal sliding through the formation of cavities (Fowler, 1986, 1987; Gagliardini et al., 2007; Iken, 1981; Lliboutry, 1959, 1968; Schoof, 2005). These cavities are assumed to reside at equilibrium with a spatially homogeneous water pressure, itself primarily imposed by surface melt and potentially modulated by the formation and evolution of subglacial channels (Röthlisberger, 1972; Schoof, 2010; Zwally et al., 2002). However, the assumption of a homogeneous water pressure field at the bed is challenged by the numerous observations that pressure below glaciers is highly variable in time and heterogeneous in space (Andrews et al., 2014; Iken & Bindschadler, 1986; Mathews, 1964; Meierbachtol et al., 2013; Rada & Schoof, 2018). Furthermore, the assumption that water pressure is primarily set by surface melt and is modulated by channel evolution is based on observations and theoretical considerations at seasonal timescales (Iken & Bindschadler, 1986;

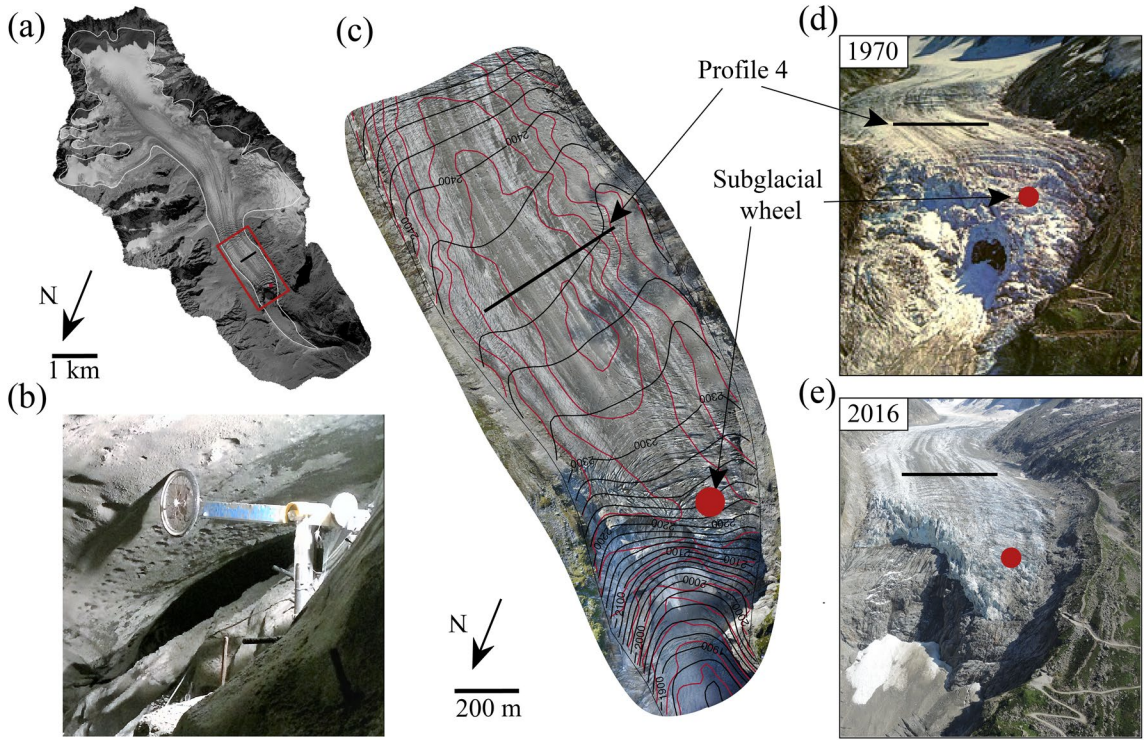

Figure 1. Pictures illustrating the Argentière Glacier setup. (a) Aerial picture of the entire glacier catchment in 2003. The white contour delineates the glacier extent. The red rectangle indicates the area shown in Figure 1c. (b) Picture of the bicycle wheel device placed in an excavated tunnel below the glacier. (c) Drone ortho-photo of the lower part of the Argentière Glacier. Red contours correspond to glacier bed topography (50 m intervals) while black contours correspond to glacier surface topography. (d) and (e): Aerial pictures of the lower part of the Argentière Glacier in 1970 and 2016. In panels (a), (c)–(e), the red dot indicates the location of the subglacial wheel, and the black line indicates the location of "profile 4", where glacier elevation measurements are made.

Schoof, 2010; Zwally et al., 2002). However, this assumption has not been fully verified over longer climatic timescales during which glacier geometry also varies significantly (Tedstone et al., 2015; Williams et al., 2020).

In addition to assumptions in theories being questionable, predictions using these are particularly challenging to test at the natural scale. Since basal physics is challenging to observe in-situ, common approaches involve the use of remote sensing observations of glacier surface velocities (Dehecq et al., 2019) often combined with numerical inversions of bed shear stress and basal velocity (Gillet-Chaulet et al., 2016; Maier et al., 2021; Minchew et al., 2016; Stearns & Veen, 2018). However, indirect inference of basal sliding velocities and limited temporal coverage of surface speeds and elevation can introduce significant uncertainties. Moreover, the reduced timespan provided by these approaches (months up to few years) often limits the analysis to hydrologically driven seasonal velocity variations (Andrews et al., 2014; Bartholomew et al., 2010; Zwally et al., 2002). These velocity variations are difficult to compare with quantifiable changes in hydrologically driven basal stresses (water pressure and bed shear stress), since local measurements are hardly representative as a result of basal hydrology being strongly heterogeneous (Rada & Schoof, 2018).

Here we use multi-decadal (1990–2019) measurements of basal sliding velocity u_b acquired from a subglacial wheel placed within an excavated tunnel under the Argentière Glacier located in the French Alps (Figure 1). Previous investigations indicate this glacier is a typical hard-bedded glacier (Vincent & Moreau, 2016; Vivian & Bocquet, 1973). Using the measured glacier thinning that operated over the three-decade period (Figures 1d and 1e, thickness has decreased from 85 to 55 m at the wheel location), we estimate the associated changes in bed shear stress and compare them to the measured changes in sliding velocity. This approach allows us to obtain an observationally derived friction law and compare it against theoretical predictions over climatic timescales.

2. Observations and Methods

2.1. Sliding Velocity Observations

Basal sliding was directly measured at the base of the glacier with an analog recording system from 1990 to 2018 (velocity was measured daily off paper drum recording) and with a digital recorder since 2018 (sampled at a 30 min interval). We show the velocity time series in Figure 2a, at the minimum daily resolution (see gray line) and filtered using a monthly moving-mean window (see colored time series). We note that we use data interpolation to fill day- to week- long data gaps as well as to correct for spurious velocity fluctuations occurring in the first two months of the time period (Supporting Information and Figure S1). We observe clear seasonal variations in sliding speed occurring as a result of summer melt water input that match an associated increase in water runoff, where runoff is measured at the outlet by the hydroelectric power company Emosson (Supporting Information and Figure S2). We also observe a long-term (multi-decadal) decrease in sliding that is well correlated with the associated glacier thinning (Vincent & Moreau, 2016). Below we detail our methodology to establish a glacier bed friction law using these long-term observations.

2.2. Methodology

2.2.1. Strategy for Establishing an Observationally Derived Glacier Bed Friction Law

Establishing an observationally derived glacier bed friction law requires evaluating changes in basal velocity u_b against changes in basal shear stress τ_b and effective pressure $N = p_i - p_w$, where p_i and p_w are ice and water pressures, respectively. Given that there exist no long-term observational constraints on p_w and thus N near our site, our approach consists in first comparing the long-term changes measured in u_b with those inferred in τ_b from the glacier geometry, and then drawing conclusions on the behavior of N based on our observational findings.

We quantify friction under two main assumptions. First, we assume that the locally observed changes in u_b reflect changes occurring at a larger scale representative of bed friction, which we refer to as the meso-scale (defined as centimeters to few tens of meters). This assumption of non-local representation is supported by u_b seasonally varying (Figure 2a) despite the sliding measurements being made in a water-free cavity where local bed shear stress and local water pressure are both always equal to zero. Second, we assume that the multi-year to multi-decadal changes in u_b are caused primarily by bed shear stress changes due to glacier thinning and retreat. This is inferred due to particularly large thickness changes observed over three decades, which alone result in a bed shear stress change of about 30 percent (Figure 1 and Supporting Information, see the next section for specifics about the bed shear stress estimates). Comparatively, bed shear stress changes from variable subglacial hydrology are expected to be mostly seasonal or shorter lived. In our analysis, we first remove the effect of subglacial hydrology from that of glacier-geometry changes on bed shear stress by comparing season to subsequent season changes, with the assumption that the subglacial hydrology configuration under a given season is similar across years. The effect of subglacial hydrology on friction is inferred at a later stage once the friction law is constrained based on the long-term data.

2.2.2. Estimating Bed Shear Stress Changes

We estimate the geometrically driven bed shear stress changes occurring at a meso-scale around the wheel by modeling the three dimensional balance of forces using the finite element software Elmer/Ice (Gagliardini et al., 2013). The bed and surface boundaries are constrained by a high resolution (10 m) bed Digital Elevation Model (DEM) (Gimbert et al., 2021) (Figure 1) and six surface DEMs acquired through the multi-decadal period (end of summer for given years, Supporting Information and Figure S3). This approach allows us to explicitly evaluate changes in τ_b and account for potential changes in transverse and/or longitudinal stresses that could arise from geometrically driven changes in normal stresses acting against bedrock topography features. We solve the Stokes equations using Glen's flow law assuming isotropic temperate ice, and we compute bed shear stress by adopting a common approach that assumes a linear friction law with a spatially uniform and time invariant friction coefficient (e.g., Jouvet et al., 2011). We note that the bed shear stress inferred with this method does not significantly depend on the chosen friction coefficient value or type of the friction law (Joughin et al., 2004; Minchew et al., 2016).

Interestingly, we find that τ_b as modeled at the wheel area is best correlated to the elevations measured yearly (in mid-September) at "profile 4" z_{p4} (location shown in Figure 1), with $\tau_b = 1.866\ 10^{-3}\ z_{p4} - 4.270$ MPa. Comparatively, correlations of τ_b to the glacier thickness, the surface slope or the driving stress estimated directly above the wheel are significantly lower (Figure S4). This finding may have two origins. First, surface height, surface slope, bed elevation and thus driving stress are particularly uncertain above the wheel due to the glacier being heavily crevassed in that area. Second, bed shear stress changes near the wheel may be largely affected by complex three-dimensional changes in glacier geometry occurring over a much larger area than near the wheel, to which elevations changes at "profile 4" are well representative. We thus use our empirically modeled relationship to estimate changes in τ_b via changes in z_{p4}. Although z_{p4} is measured yearly, we model the seasonal variability in z_{p4} due to winter snow accumulation and summer ablation in order to incorporate the induced seasonal variability in τ_b (Supporting Information and Figure S5).

3. Results

3.1. General Observational Features

We find distinct but remarkably well resolved relationships between u_b and τ_b over the three-decade-long period for measurements made at the annual velocity minima (large dots, Figure 2b), averaged

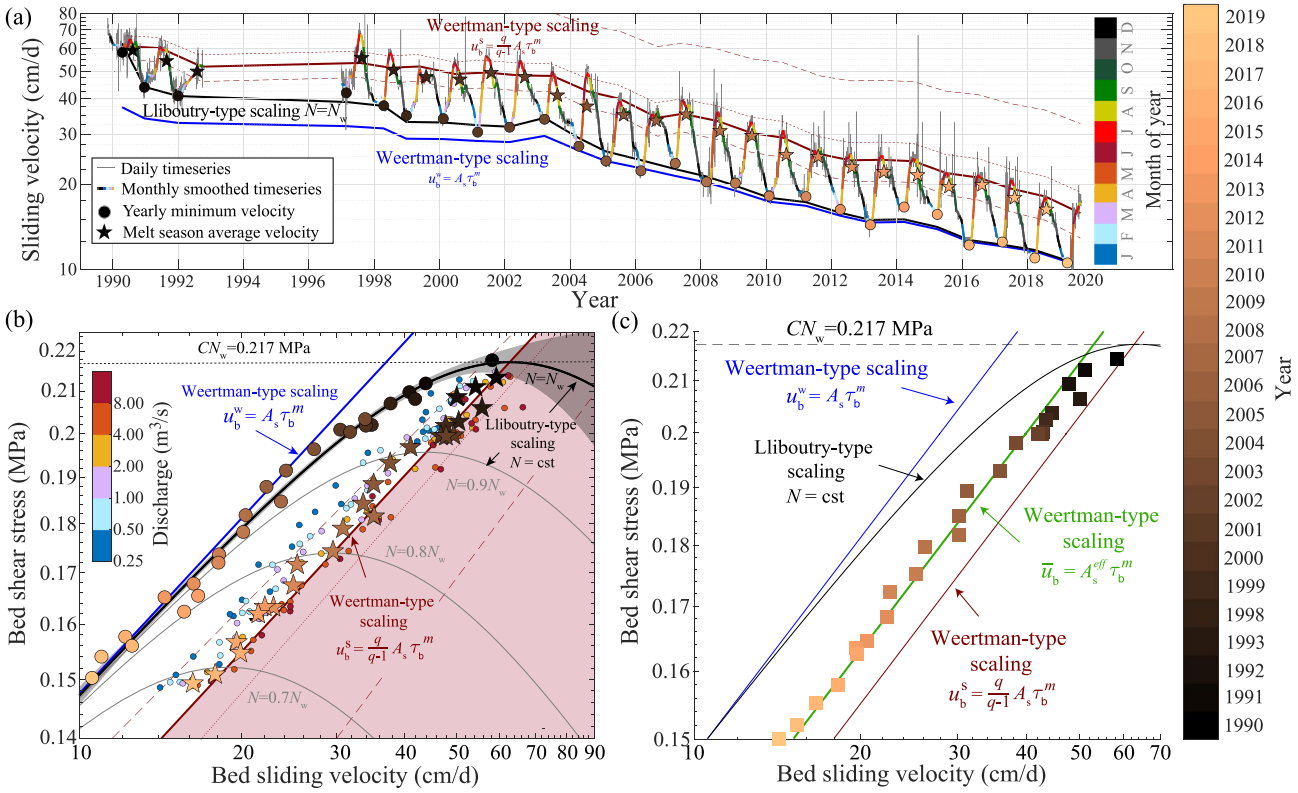

Figure 2. (a) Observed sliding velocity timeseries at daily (gray line) and monthly (colored line) resolutions and (b), (c) observed versus predicted glacier bed friction laws. (b) One-month averaged bed shear stress τ_b versus bed sliding velocity u_b for the end of winter velocity minimum (large dots), summer (stars), and at various discharges throughout summer (small dots). Predicted friction using a Weertman-type friction law (thick blue line) and the Lliboutry-type pressure-dependant friction law expressed in Equation 1 using $CN_w = 0.217$ MPa (thick black curve) and varying effective pressure N (thin gray curves). The black horizontal dashed line shows Iken's limit $\tau_b = CN_w$. The red line corresponds to the cavity-driven friction law using parameters m, A_s and q as fitted using winter minimum velocities and prescribing summer effective pressure equal to Iken's limit τ_b/C. The gray shaded area and the red dashed lines show prediction bounds associated with the continuous black and red predictions, respectively. The red dotted line shows a likely upper-bound for velocity at Iken's limit, which is obtained under the physical constraint that q is likely equal to or higher than 2. (c) τ_b versus u_b as observed using mean annual velocity and bed shear stress (squares). The green line corresponds to a simple Weertman-type friction law with $m = 3.38$ and an effective sliding parameter A_s^{eff} that is adjusted in order to generally match the observed yearly averaged velocities. The blue and red lines as well as the black curve are given as references and correspond to the predictions shown in (b).

over summer (stars, Figure 2b), and averaged over a range of emerging subglacial discharge (small dots, Figure 2b). Here, minimum velocity typically occurs at the end of February–beginning of March (Figure 2a) and summer is defined as the period during each year where the subglacial discharge is higher than 0.25 $m^3\ s^{-1}$ (typical start is end of April and typical end is early November, Figure 3a). In agreement with hard-bed theory, observations made during periods where conditions are not favorable to cavitation exhibit a Weertman-type scaling $u_b = A_s {\tau_b}^m$ (Weertman, 1957, see blue line in Figures 2b and 2a), where A_s ($m\ s^{-1}\ Pa^{-m}$) is the sliding parameter and m an exponent. This scaling is observed at the yearly minimum velocity in winter (see large dots) when water input from melt does not occur and over recent years (starting around 2005 until the present) when bed shear stress is low. Interestingly, however, such a Weertman-type scaling does not capture annual velocity minima at the higher shear stresses for which the data exhibits significant curvature, indicating frictional softening. This softening could be produced via cavitation expansion (Lliboutry, 1959, 1968), or potentially via internal ice fracturing (Walter et al., 2013). Most surprisingly, summer-averaged observations (see stars in Figure 2b), as well as observations at similar summer discharge (see small dots), also exhibit a Weertman-type scaling (see red line), even though sliding is thought to be highly modulated by cavitation during these periods, a process which is not accounted for in Weertman's theory. It is unlikely that internal ice fracturing could explain this scaling, since there is no physical reason for basal ice fracturing to exhibit a Weertman-type scaling, and no significant seasonal changes in basal seismicity are observed at the site (Helmstetter, Moreau, et al., 2015; Helmstetter, Nicolas, et al., 2015).

3.2. Constraining a Pressure-Dependent Friction Law Using Winter Observations

We compare our observations with theoretical predictions using a pressure-dependent friction law that incorporates Lliboutry's concept of cavitation (Lliboutry, 1959, 1968) and Iken's concept of bounded shear stress (Iken, 1981). A friction law that satisfies these conditions can be written as (Gagliardini et al., 2007; Helanow et al., 2020; Schoof, 2005; Zoet & Iverson, 2015, 2016)

$$\frac{\tau_b}{CN} = f(\chi) \tag{1}$$

where $f(\chi) = (\chi/(1+\alpha\chi^q))^{1/m} \leq 1$, $\chi = u_b/(C^m N^m A_s)$, $\alpha = (q-1)^{q-1}/q^q$, C is a Coulomb-type friction coefficient and q is a bed-shape exponent ≥1. This relationship predicts curvature in the τ_b versus u_b logarithmic space if N is constant, such that τ_b/CN varies. On the opposite, this relationship predicts a Weertman-like power law relationship (i.e., no curvature in the τ_b versus u_b logarithmic space) if N scales with τ_b, such that τ_b/CN is constant. We find that this friction law is best constrained from fitting winter minimum velocity observations and prescribing winter effective pressure N_w as a constant, which gives $m = 3.38 \pm 0.42$, $A_s = 2.35.10^4$ $(0.1–5.9).10^4\ m\ yr^{-1}\ MPa^{-m}$, $q = 2.44 \pm 1.07$ and $CN_w = 0.217 \pm 0.02$ MPa (black line in Figures 2b and 2a, see Supporting Information for the uncertainty calculations). The condition that N_w remains constant under changing ice thickness can be explained by basal water pressure being controlled by subglacial water flowing through conduits at equilibrium in winter (Supporting Information). Similar values of A_s and q are obtained from surface velocity observations in 2018–2019 at "profile 4" where the surface gradient is much lower (10% instead of 20%) and the ice is much thicker (250 m instead of 55 m) (Supporting Information). These similarities support the contention that our inferred friction law is likely representative of a large part of the glacier. The inferred value of $m = 3.38 \pm 0.42$ is in striking agreement with Weertman's theory considering that enhanced creep solely controls friction, in which case m equals the Glen's flow law exponent $n \approx 3–4$ (Cuffey & Paterson, 2010) as opposed to m equals $(n+1)/2 \approx 2–2.5$ if regelation also plays a role (Weertman, 1957). The inferred value of $q = 2.44 \pm 1.07$ is also consistent with expectations from numerical simulations (Gagliardini et al., 2007), although the associated uncertainty is large. In fact, we note that low q-values (e.g., lower than 2, see red dotted line in Figures 2a and 2b) are generally not expected since they require a bed roughness topography exhibiting sharp slope changes (i.e., a sawtooth-like bedrock, see Gagliardini et al., 2007) that would likely be smoothed by preferential erosion due to stress concentration at these locations (Hallet, 1996). N_w that is lower than or equal to ice pressure implies that the friction coefficient C is higher than or equal to 0.25. We estimate $C \approx 0.4$ using a 9 bar water pressure that was measured during the winter 1968 (Vivian & Zumstein, 1969) when the glacier had a similar geometry to that in 1990 (Vincent et al., 2009). Observations can match the predictions without the need for explicitly describing

extra friction exerted from sediments or from other potential mechanisms at the source of basal stick-slip seismic events (Helmstetter, Nicolas, et al., 2015; Lipovsky et al., 2019).

3.3. Understanding Summer Observations

Interestingly, the cavity-driven friction law as fitted using the annual minimum velocity observations strikingly predicts summer observations if summer effective pressure is set to scale with bed shear stress and in particular to Iken's limit τ_b/C (keeping values of m, A_s and q equal to those inferred based on fitting winter minimum velocity data). In this case summer sliding velocity u_b^s Equation 1 simplifies to a Weertman-type law of the form $u_b^s = q/(q-1)A_s\tau_b^m$ (red continuous line in Figure 2b, see also Figure 2a). Thus, we find that Iken's limit is approached at winter minimum velocity in 1990 but also every subsequent summer (Figures 2b and 3b) when subglacial hydrology is subjected to significant and highly fluctuating water input from surface melt. This finding demonstrates that multi-decadal changes in sliding velocities are not significantly affected by short-term, melt- or precipitation-induced sliding speed variations (Vincent and Moreau, 2016), under which sliding speed is much higher than that predicted using $u_b^s = q/(q-1)A_s\tau_b^m$. It also suggests that Iken's limit is approached over any portion of the glacier bed that is subjected to water input from surface melt, since

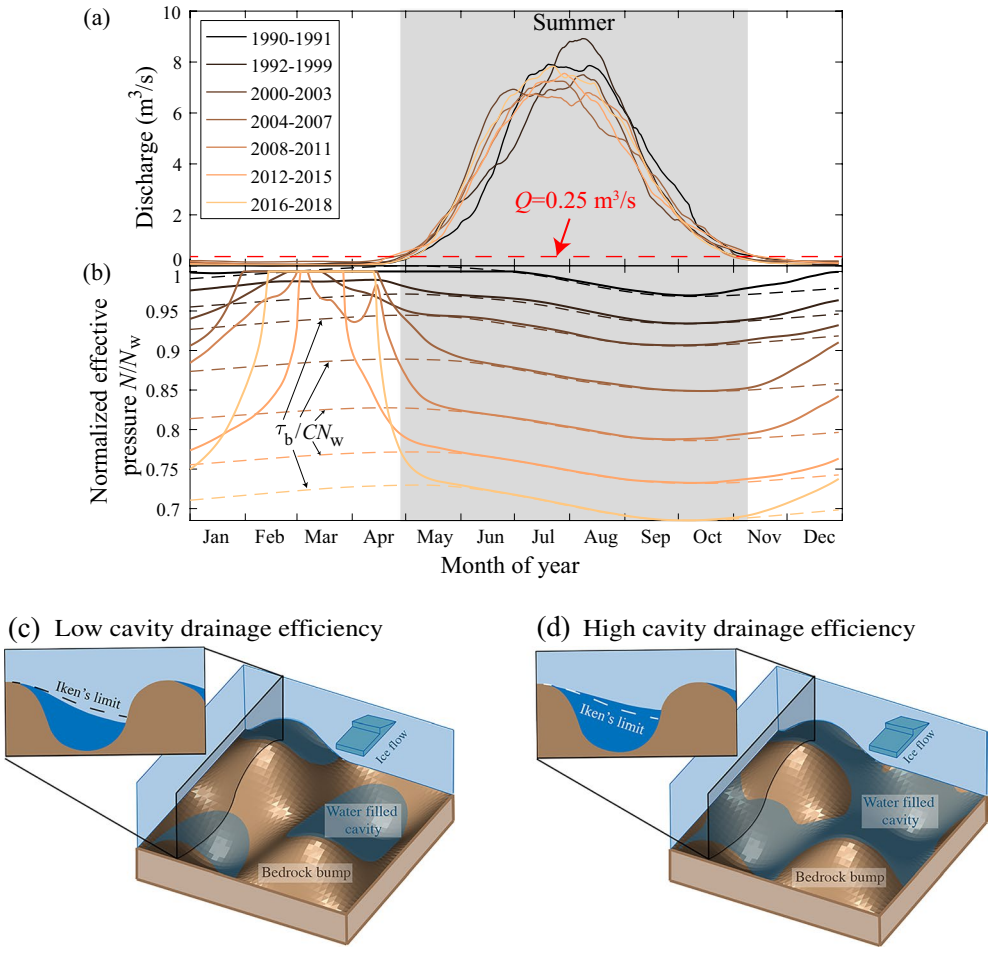

Figure 3. Seasonal variations of (a) discharge and (b) normalized effective pressure N/N_w for various time periods (see colorscale). The normalized effective pressure N/N_w is inverted using Equation 1 (with parameters m, A_s and q obtained from fitting winter minimum velocity data, Figure 2b) and the observed seasonal variations in sliding velocity and bed shear stress. All timeseries are smoothed at a monthly timescale. The red dashed line in (a) shows the discharge threshold used to define the summer period. Dashed lines in (b) indicate predictions of the normalized Iken's limit τ_b/CN_w. (c) and (d) Two- and three-dimensional cartoons illustrating the cavitation stage and drainage capacity increase through cavity connection near Iken's limit.

summer bed stress conditions consistently lie near Iken's limit regardless of bed shear stress over a wide range of subglacial discharges (from 0.25 to 0.4 $m^3\ s^{-1}$, see blue dots, to more than 8 $m^3\ s^{-1}$, see red dots in Figure 2b and also Figure 3b). Given this behavior, we posit there must exist a stabilizing mechanism inherent to the friction process that maintains glacier basal sliding velocities near those at Iken's limit. This mechanism potentially prevents sliding to enter the velocity-weakening regime, in which shear stress decreases with sliding velocity (Gagliardini et al., 2007; Helanow et al., 2020; Iken, 1981; Schoof, 2005; Zoet & Iverson, 2015) and the glacier is prone to instability (Minchew & Meyer, 2020; Thøgersen et al., 2019). We find this mechanism causes the effective pressure to scale with bed shear stress (Figure 3b), as opposed to independently varying as water supply variability and drainage conditions change (Andrews et al., 2014; Hoffman et al., 2016; Schoof, 2010; Zwally et al., 2002). Further, this mechanism exerts a primary control in the overall glacier dynamics, since it causes year-averaged velocities to follow a Weertman-type scaling with exponent $m \approx 3.38$ rather than a more complex law (Gagliardini et al., 2007; Schoof, 2005; Zoet & Iverson, 2020) (Figure 2c).

4. Discussion

4.1. Stabilization Near Iken's Limit

We propose that stabilization near Iken's limit results from a positive feedback between bed sliding velocity and water drainage efficiency throughout the cavity network that acts to halt further cavity expansion. Enhanced sliding results in enlarged cavities and thus a drawdown of water pressure, helping to prevent further expansion of the cavities (Hewitt, 2013; Hoffman & Price, 2014) and ensuring stable sliding. Stabilization must occur at the level of cavitation, and thus sliding velocity, at which the drainage efficiency set by cavity network connectivity (Andrews et al., 2014; Hoffman et al., 2016; Iken & Bindschadler, 1986; Kamb, 1987) accommodates the meltwater supply. For stabilization to occur near Iken's limit regardless of the average water input rate (i.e., the average emerging water discharge, see Figures 2b and 3b), drainage efficiency must be low under stress conditions below Iken's limit but must increase drastically as stress conditions approach Iken's limit. This behavior may be explained by ice-bed separation over cavity crests strongly increasing near Iken's limit under realistic three-dimensional bed geometries (see Figures 3c and 3d). This is consistent with sliding-induced cavitation rather than orifices (Kamb, 1987) being the main control on hydrologic connections between cavities. The hydrology-cavity feedback identified here may prevent instability to occur as bed stresses approach Iken's limit for glaciers over hard bed. However, this feedback may no longer operate for glaciers over soft bed, since cavitation may not play an important role in that case. This might serve as an explanation for why glacier surges are primarily observed on till-bedded glaciers (Cuffey & Paterson, 2010).

4.2. On the Use of a Simple Weertman-Type Scaling to Predict Long Term Sliding Velocity Changes

Sliding velocities may follow a Weertman-type scaling as long as the hydrology-cavity feedback controls effective pressure, making it scale with bed shear stress. This requires water to be primarily drained through a network of cavities. We suggest that this condition is fulfilled over the area controlling friction near the wheel and in summer as a result of water input from surface melt being widely distributed into the numerous crevasses (Veen, 2007) (see Figures 1c–1e and Figure S3). In this scenario, the general water throughput rate is sufficiently low for channels to not form, and thus water is conveyed through cavities from the input location to either a main drainage channel near the glacier axis, or the glacier outlet. Sliding velocities are expected to depart from a Weertman-type scaling if effective pressure is not governed by the hydrology-cavity feedback. This is expected along margins of marine terminating glaciers where ocean-induced buoyancy may control effective pressure, consistent with observations that suggest a Weertman-type scaling does not hold in these regions (Stearns & Veen, 2018). Deviation from a Weertman-type scaling is also expected where melt water throughput rates are sufficient for channels to form near input locations and thus channelized drainage exerts primary control on the overall effective pressure field (Röthlisberger, 1972; Schoof, 2010). Observations on mountain glaciers (Lambrecht et al., 2014; Mair et al., 2003; Nienow et al., 1998; Scherler & Strecker, 2012) and from land-terminating regions of Greenland (Bartholomew et al., 2010; Chandler et al., 2013; Sole et al., 2013; Tedstone et al., 2013; Zwally et al., 2002) suggest that channelized drainage may modulate effective pressure during late summer. However, this only occurs during a

small fraction of the year corresponding to a few months when melt rates are high and channels have had sufficient time to fully develop. Other observations suggest channelization does not play a main role in summer dynamics. In Greenland basal water pressures are often unfavorable to channel development more than a few tens of kilometers away from the margin (Meierbachtol et al., 2013), the seasonal glacier slowdown attributed to channelization is often not observed on marine-terminating glaciers (Moon et al., 2014), and evolving drainage efficiency in the non-channelized system is thought to be the main control on late summer flow speeds (Andrews et al., 2014). Thus, while our data is limited to one particular glacier, it seems possible and consistent with other available data that the hydrology-cavity feedback identified with our observations could also have a prominent role in controlling year-averaged effective pressure and thus basal motion on large ice sheets and ice caps. We show that regions satisfying these conditions would likely exhibit a simple Weertman-type scaling with exponent $m \approx 3$–4, as recently observed on Himalayan Glaciers (Dehecq et al., 2019) and in most places across the Greenland Ice-Sheet (Maier et al., 2021). Given these evidences, our findings could help significantly reduce the complexity of predicting glaciers and ice-sheets dynamics into the future (Brondex et al., 2017; Joughin et al., 2019; Ritz et al., 2015).

5. Conclusions

We analyze unique observations of sliding velocity and bed shear stress changes below a hard-bed glacier in the French Alps. We demonstrate that these observations combined allow us to test the basic components of existing hard-bed friction theories, and to identify novel mechanisms that control friction. In striking agreement with theory, we observe a Weertman-type scaling at low shear stresses and a transition to a Lliboutry-type scaling at higher shear stresses, consistent with subglacial cavity growth and Iken's concept of bounded shear stress. Surprisingly, however, glacier basal stress conditions are observed to stabilize every summer near Iken's limit, which causes effective pressure to scale with bed shear stress. This finding challenges the notion of effective pressure being solely a complex function of melt water input and evolving drainage as commonly thought. The occurrence of such a stabilization mechanism causes the year-averaged velocities to follow a Weertman-type scaling rather than more complex ones, which have been defined on the presently challenged premise that effective pressure varies independently of bed shear stress. While it remains to be verified whether this hydrology-cavity feedback occurs in other settings like Greenland, current evidence suggests this stabilization mechanism could be widely operational. Thus, our findings have the potential to strongly simplify predicting hard-bedded glaciers response to climate change and to reduce uncertainty in projections of sea-level rise.

Data Availability Statement

The datasets generated and/or analyzed in the current study are available on the repository platform Zenodo at the following link: https://doi.org/10.5281/zenodo.4286111.

Acknowledgments
This work is supported by the French ANR project SAUSSURE (ANR-18-CE01-0015-01). The authors thank the Electricité Emosson SA hydropower company for providing subglacial discharge measurements. Surface DEMs have been provided by the French National Geographic Institute (IGN) for year 1979, and by the European Facility for Airborne Research Transnational Access for year 2015. Glacier surface elevation at "profile 4" was measured in the framework of the GLACIOCLIM program (https://glacioclim.osug.fr). The authors thank numerous anonymous reviewers who commented on the present as well as previous versions of this manuscript, and Nathan Maier for fruitful discussions and edit suggestions.

References

Andrews, L. C., Catania, G. A., Hoffman, M. J., Gulley, J. D., Lüthi, M. P., Ryser, C., et al. (2014). Direct observations of evolving subglacial drainage beneath the Greenland ice sheet. *Nature*, *514*(7520), 80–83. https://doi.org/10.1038/nature13796

Bartholomew, I., Nienow, P., Mair, D., Hubbard, A., King, M. A., & Sole, A. (2010). Seasonal evolution of subglacial drainage and acceleration in a Greenland outlet glacier. *Nature Geoscience*, *3*(6), 408–411. https://doi.org/10.1038/ngeo863

Brondex, J., Gagliardini, O., Gillet-Chaulet, F., & Durand, G. (2017). Sensitivity of grounding line dynamics to the choice of the friction law. *Journal of Glaciology*, *63*(241), 854–866. https://doi.org/10.1017/jog.2017.51

Chandler, D. M., Wadham, J. L., Lis, G. P., Cowton, T., Sole, A., Bartholomew, I., et al. (2013). Evolution of the subglacial drainage system beneath the Greenland ice sheet revealed by tracers. *Nature Geoscience*, *6*(3), 195–198. https://doi.org/10.1038/ngeo1737

Cuffey, K. M., & Paterson, W. S. B. (2010). *The physics of glaciers* (4th ed.). Burlington, MA, USA: Butterworth-Heinemann.

Dehecq, A., Gourmelen, N., Gardner, A. S., Brun, F., Goldberg, D., Nienow, P. W., et al. (2019). Twenty-first century glacier slowdown driven by mass loss in High Mountain Asia. *Nature Geoscience*, *12*(1), 22–27. https://doi.org/10.1038/s41561-018-0271-9

Fowler, A. C. (1986). A sliding law for glaciers of constant viscosity in the presence of subglacial cavitation. *Proceedings of the Royal Society of London. A. Mathematical and Physical Sciences*, *407*(1832), 147–170. https://doi.org/10.1098/rspa.1986.0090

Fowler, A. C. (1987). Sliding with cavity formation. *Journal of Glaciology*, *33*(115), 255–267. https://doi.org/10.3189/S0022143000008820

Gagliardini, O., Cohen, D., Råback, P., & Zwinger, T. (2007). Finite-element modeling of subglacial cavities and related friction law. *Journal of Geophysical Research*, *112*(F2), F02027. https://doi.org/10.1029/2006JF000576

Gagliardini, O., Zwinger, T., Gillet-Chaulet, F., Durand, G., Favier, L., Fleurian, B., et al. (2013). Capabilities and performance of Elmer/Ice, a new-generation ice sheet model. *Geoscientific Model Development*, *6*(4), 1299–1318. https://doi.org/10.5194/gmd-6-1299-2013

Gillet-Chaulet, F., Durand, G., Gagliardini, O., Mosbeux, C., Mouginot, J., Rémy, F., & Ritz, C. (2016). Assimilation of surface velocities acquired between 1996 and 2010 to constrain the form of the basal friction law under Pine island glacier. *Geophysical Research Letters*, *43*(19), 10311–10321. https://doi.org/10.1002/2016GL069937

Gimbert, F., Nanni, U., Roux, P., Helmstetter, A., Garambois, S., Lecointre, A., et al. (2021). A multi-physics experiment with a temporary dense seismic array on the Argentière glacier, french Alps: The RESOLVE project. *Seismological Research Letters*, *92*, 1185–1201. https://doi.org/10.1785/0220200280

Hallet, B. (1996). Glacial quarrying: A simple theoretical model. *Annals of Glaciology*, *22*, 1–8. https://doi.org/10.3189/1996AoG22-1-1-8

Helanow, C., Iverson, N. R., Zoet, L. K., & Gagliardini, O. (2020). Sliding relations for glacier slip with cavities over three-dimensional beds. *Geophysical Research Letters*, *47*(3), e2019GL084924. https://doi.org/10.1029/2019GL084924

Helmstetter, A., Moreau, L., Nicolas, B., Comon, P., & Gay, M. (2015). Intermediate-depth icequakes and harmonic tremor in an Alpine glacier (Glacier d'Argentière, France): Evidence for hydraulic fracturing? *Journal of Geophysical Research: Earth Surface*, *120*(3), JF003289. https://doi.org/10.1002/2014JF003289

Helmstetter, A., Nicolas, B., Comon, P., & Gay, M. (2015). Basal icequakes recorded beneath an Alpine glacier (Glacier d'Argentière, Mont Blanc, France): Evidence for stick-slip motion? *Journal of Geophysical Research: Earth Surface*, *120*(3), JF003288. https://doi.org/10.1002/2014JF003288

Hewitt, I. J. (2013). Seasonal changes in ice sheet motion due to melt water lubrication. *Earth and Planetary Science Letters*, *371–372*, 16–25. https://doi.org/10.1016/j.epsl.2013.04.022

Hoffman, M., & Price, S. (2014). Feedbacks between coupled subglacial hydrology and glacier dynamics. *Journal of Geophysical Research: Earth Surface*, *119*(3), 414–436. https://doi.org/10.1002/2013JF002943

Hoffman, M. J., Andrews, L. C., Price, S. F., Catania, G. A., Neumann, T. A., Lüthi, M. P., et al. (2016). Greenland subglacial drainage evolution regulated by weakly connected regions of the bed. *Nature Communications*, *7*(1), 1–12. https://doi.org/10.1038/ncomms13903

Iken, A. (1981). The effect of the subglacial water pressure on the sliding velocity of a glacier in an idealized numerical model. *Journal of Glaciology*, *27*(97), 407–421. https://doi.org/10.3189/S0022143000011448

Iken, A., & Bindschadler, R. A. (1986). Combined measurements of subglacial water pressure and surface velocity of Findelengletscher, Switzerland: Conclusions about drainage system and sliding mechanism. *Journal of Glaciology*, *32*(110), 101–119. https://doi.org/10.3189/S0022143000006936

Joughin, I., MacAyeal, D. R., & Tulaczyk, S. (2004). Basal shear stress of the ross ice streams from control method inversions. *Journal of Geophysical Research*, *109*(B9), B09405. https://doi.org/10.1029/2003JB002960

Joughin, I., Smith, B. E., & Schoof, C. G. (2019). Regularized coulomb friction laws for ice sheet sliding: Application to Pine island glacier, Antarctica. *Geophysical Research Letters*, *46*(9), 4764–4771. https://doi.org/10.1029/2019GL082526

Jouvet, G., Huss, M., Funk, M., & Blatter, H. (2011). Modelling the retreat of Grosser Aletschgletscher, Switzerland, in a changing climate. *Journal of Glaciology*, *57*(206), 1033–1045. https://doi.org/10.3189/002214311798843359

Kamb, B. (1987). Glacier surge mechanism based on linked cavity configuration of the basal water conduit system. *Journal of Geophysical Research*, *92*(B9), 9083–9100. https://doi.org/10.1029/JB092iB09p09083

Lambrecht, A., Mayer, C., Aizen, V., Floricioiu, D., & Surazakov, A. (2014). The evolution of Fedchenko glacier in the Pamir, Tajikistan, during the past eight decades. *Journal of Glaciology*, *60*(220), 233–244. https://doi.org/10.3189/2014JoG13J110

Lipovsky, B. P., Meyer, C. R., Zoet, L. K., McCarthy, C., Hansen, D. D., Rempel, A. W., & Gimbert, F. (2019). Glacier sliding, seismicity and sediment entrainment. *Annals of Glaciology*, *60*, 1–11. https://doi.org/10.1017/aog.2019.24

Lliboutry, L. (1959). Une théorie du frottement du glacier sur son lit. *Annales de Geophysique*, *15*, 250–256.

Lliboutry, L. (1968). General theory of subglacial cavitation and sliding of temperate glaciers. *Journal of Glaciology*, *7*, 21–58.

Maier, N., Gimbert, F., Gillet-Chaulet, F., & Gilbert, A. (2021). Basal traction mainly dictated by hard-bed physics over grounded regions of Greenland. *The Cryosphere*, *15*(3), 1435–1451. https://doi.org/10.5194/tc-15-1435-2021

Mair, D., Willis, I., Fischer, U. H., Hubbard, B., Nienow, P., & Hubbard, A. (2003). Hydrological controls on patterns of surface, internal and basal motion during three "spring events": Haut Glacier d'Arolla, Switzerland. *Journal of Glaciology*, *49*(167), 555–567. https://doi.org/10.3189/172756503781830467

Mathews, W. H. (1964). Water pressure under a glacier. *Journal of Glaciology*, *5*(38), 235–240.

Meierbachtol, T., Harper, J., & Humphrey, N. (2013). Basal drainage system response to increasing surface melt on the Greenland ice sheet. *Science*, *341*(6147), 777–779. https://doi.org/10.1126/science.1235905

Minchew, B., & Meyer, C. R. (2020). Dilation of subglacial sediment governs incipient surge motion in glaciers with deformable beds. *Proceedings of the Royal Society A: Mathematical, Physical & Engineering Sciences*, *476*(2238), 20200033. https://doi.org/10.1098/rspa.2020.0033

Minchew, B., Simons, M., Björnsson, H., Pálsson, F., Morlighem, M., Seroussi, H., et al. (2016). Plastic bed beneath Hofsjökull Ice Cap, central Iceland, and the sensitivity of ice flow to surface meltwater flux. *Journal of Glaciology*, *62*(231), 147–158. https://doi.org/10.1017/jog.2016.26

Moon, T., Joughin, I., Smith, B., Broeke, M. R., Berg, W. J., Noël, B., & Usher, M. (2014). Distinct patterns of seasonal Greenland glacier velocity. *Geophysical Research Letters*, *41*(20), 7209–7216. https://doi.org/10.1002/2014GL061836

Nienow, P., Sharp, M., & Willis, I. (1998). Seasonal changes in the morphology of the subglacial drainage system, Haut Glacier d'Arolla, Switzerland. *Earth Surface Processes and Landforms*, *23*(9), 825–843. https://doi.org/10.1002/(SICI)1096-9837(199809)23:9<825::AID-ESP893>3.0.CO;2-2

Rada, C., & Schoof, C. (2018). Channelized, distributed, and disconnected: Subglacial drainage under a valley glacier in the Yukon. *The Cryosphere*, *12*(8), 2609–2636. https://doi.org/10.5194/tc-12-2609-2018

Ritz, C., Edwards, T. L., Durand, G., Payne, A. J., Peyaud, V., & Hindmarsh, R. C. A. (2015). Potential sea-level rise from Antarctic ice-sheet instability constrained by observations. *Nature*, *528*(7580), 115–118. https://doi.org/10.1038/nature16147

Röthlisberger, H. (1972). Water pressure in intra- and subglacial channels *. *Journal of Glaciology*, *11*(62), 177–203. https://doi.org/10.3189/S0022143000022188

Scherler, D., & Strecker, M. R. (2012). Large surface velocity fluctuations of Biafo glacier, central Karakoram, at high spatial and temporal resolution from optical satellite images. *Journal of Glaciology*, *58*(209), 569–580. https://doi.org/10.3189/2012JoG11J096

Schoof, C. (2005). The effect of cavitation on glacier sliding. *Proceedings of the Royal Society of London: Mathematical, Physical and Engineering Sciences*, *461*(2055), 609–627. https://doi.org/10.1098/rspa.2004.1350

Schoof, C. (2010). Ice-sheet acceleration driven by melt supply variability. *Nature*, *468*(7325), 803–806. https://doi.org/10.1038/nature09618

Smith, A. M. (2006). Microearthquakes and subglacial conditions. *Geophysical Research Letters*, *33*(24), L24501. https://doi.org/10.1029/2006GL028207

Sole, A., Nienow, P., Bartholomew, I., Mair, D., Cowton, T., Tedstone, A. J., & King, M. A. (2013). Winter motion mediates dynamic response of the Greenland ice sheet to warmer summers. *Geophysical Research Letters*, *40*(15), 3940–3944. https://doi.org/10.1002/grl.50764

Stearns, L. A., & Veen, C. J. (2018). Friction at the bed does not control fast glacier flow. *Science*, *361*(6399), 273–277. https://doi.org/10.1126/science.aat2217

Tedstone, A. J., Nienow, P. W., Gourmelen, N., Dehecq, A., Goldberg, D., & Hanna, E. (2015). Decadal slowdown of a land-terminating sector of the Greenland ice sheet despite warming. *Nature*, *526*(7575), 692–695. https://doi.org/10.1038/nature15722

Tedstone, A. J., Nienow, P. W., Sole, A. J., Mair, D. W. F., Cowton, T. R., Bartholomew, I. D., & King, M. A. (2013). Greenland ice sheet motion insensitive to exceptional meltwater forcing. *Proceedings of the National Academy of Sciences*, *110*(49), 19719–19724. https://doi.org/10.1073/pnas.1315843110

Thøgersen, K., Gilbert, A., Schuler, T. V., & Malthe-Sørenssen, A. (2019). Rate-and-state friction explains glacier surge propagation. *Nature Communications*, *10*(1), 1–8. https://doi.org/10.1038/s41467-019-10506-4

Veen, C. J. (2007). Fracture propagation as means of rapidly transferring surface meltwater to the base of glaciers. *Geophysical Research Letters*, *34*(1), L01501. https://doi.org/10.1029/2006GL028385

Vincent, C., & Moreau, L. (2016). Sliding velocity fluctuations and subglacial hydrology over the last two decades on Argentière glacier, Mont Blanc area. *Journal of Glaciology*, *62*, 805–815. https://doi.org/10.1017/jog.2016.35

Vincent, C., Soruco, A., Six, D., & Meur, E. L. (2009). Glacier thickening and decay analysis from 50 years of glaciological observations performed on Glacier d'Argentière, Mont Blanc area, France. *Annals of Glaciology*, *50*(50), 73–79. https://doi.org/10.3189/172756409787769500

Vivian, R., & Bocquet, G. (1973). Subglacial cavitation phenomena under the glacier D'Argentière, Mont Blanc, France. *Journal of Glaciology*, *12*(66), 439–451. https://doi.org/10.3189/S0022143000031853

Vivian, R. A., & Zumstein, J. (1969). Hydrologie sous-glaciaire au glacier d'Argentière (Mont-Blanc, France). *Journal of Glaciology*, *12*, 53–64.

Walter, F., Dalban Canassy, P., Husen, S., & Clinton, J. F. (2013). Deep icequakes: What happens at the base of Alpine glaciers? *Journal of Geophysical Research: Earth Surface*, *118*(3), 1720–1728. https://doi.org/10.1002/jgrf.20124

Weertman, J. (1957). On the sliding of glaciers. *Journal of Glaciology*, *3*(21), 33–38. https://doi.org/10.3189/S0022143000024709

Williams, J. J., Gourmelen, N., & Nienow, P. (2020). Dynamic response of the Greenland ice sheet to recent cooling. *Scientific Reports*, *10*(1), 1647. https://doi.org/10.1038/s41598-020-58355-2

Zoet, L. K., & Iverson, N. R. (2015). Experimental determination of a double-valued drag relationship for glacier sliding. *Journal of Glaciology*, *61*(225), 1–7. https://doi.org/10.3189/2015JoG14J174

Zoet, L. K., & Iverson, N. R. (2016). Rate-weakening drag during glacier sliding. *Journal of Geophysical Research: Earth Surface*, *121*(7), 1206–1217. https://doi.org/10.1002/2016JF003909

Zoet, L. K., & Iverson, N. R. (2020). A slip law for glaciers on deformable beds. *Science*, *368*(6486), 76–78. https://doi.org/10.1126/science.aaz1183

Zwally, H. J., Abdalati, W., Herring, T., Larson, K., Saba, J., & Steffen, K. (2002). Surface melt-induced acceleration of Greenland ice-sheet flow. *Science*, *297*(5579), 218–222. https://doi.org/10.1126/science.1072708